High-Resolution EPR and Quantum Effects on CH_3, CH_2D, CHD_2, and CD_3 Radicals under Argon Matrix Isolation Conditions

Tomoya Yamada,[†] Kenji Komaguchi,[†] Masaru Shiotani,[†] Nikolas P. Benetis,*[,‡] and Anders R. Sørnes[§]

Department of Applied Chemistry, Faculty of Engineering, Hiroshima University, Higashi-Hiroshima 739-8527, Japan, Department of Physics IFM, Chemical Physics, Linköping University, S-581 83 Linköping, Sweden, and Department of Physics, University of Oslo, P.O. Box 1048 Blindern, N-0316 Oslo, Norway

Received: December 10, 1998; In Final Form: March 25, 1999

High-resolution EPR spectra of CH_3, $^{13}CH_3$, and even CH_2D radicals with their natural abundances have been observed in Ar matrix in the temperature range 4.2−40 K. This was achieved by X-ray radiolysis of Ar matrix containing 0.2 mol % CH_4. The high-resolution EPR spectra of CD_3 and CHD_2 radicals were also obtained under similar conditions using CD_4 and CH_2D_2 instead of CH_4, respectively. At the lower temperatures, the EPR line shapes of these radicals are dominated by hyperfine (hf) patterns with anomalous intensity, attributed to quantum effects. The application of the Pauli principle in combination with D_3 point-group symmetry results in interesting exclusion of EPR transitions for both the α-proton- and the α-deuteron-rotor spectra. In contrast to the β-proton methyls $>\dot{C}-CH_3$, the hf coupling is anisotropic and no rotation-hindering barrier is present here. The "E" lines of the corresponding isotropic β-proton methyl rotor [Sørnes, A. R.; Benetis, N. P. *Chem. Phys.* **1998**, *226*, 151][1] are absent from their regular positions. The deuteron rotor is giving a peculiar spectrum at the lowest experimental temperature, i.e., an extremely strong central singlet superimposed on a much weaker fast motional spectrum. The quantum effects are attributed to spin-rotation coupling through the anisotropic part of the hf interaction and exchange symmetry of at least two identical fermions or bosons of the studied radicals. The experimental findings are consistent with a three-dimensional, free quantum-rotor motional model.

1. Introduction

Since EPR spectroscopy of radicals generated by ionizing radiation of organic compounds have been established, a number of EPR studies have been carried out concerning methyl radicals isolated in inert gas matrixes,[2−5] adsorbed on solid surfaces,[6,7] and trapped in organic media[8,9] at low temperatures. Most theoretical studies of quantum effects on EPR line shapes of methyl-type rotors so far have been concentrated in isotropic hyperfine (hf) interactions and strongly hindered rotation. As such systems, the EPR spectra of $>\dot{C}-CH_3$ radical (β-proton methyl rotor)[1,9,10] at low temperatures near 4 K are well-known to consist of a quartet with equal intensity 1:1:1:1 and hf splitting of ca. 2.3 mT, instead of following the binomial intensity distribution 1:3:3:1. This line shape has been explained theoretically by McConnell.[11] The equal intensity of the four lines was attributed to quantum tunneling effects. The tunneling allows for rotation of the radical about its C_3 molecular axis even at the lowest torsional state. That is, since torsion is coupled with the nuclear spin, the population at lowest mixed spin-rotational "A" state is reflected in the spectrum. In such a tunneling rotation, not only the "A" state but also the "E" nuclear spin states appear by considering the next higher rotational levels. The EPR transitions corresponding to these states, however, have not been discussed previously for isolated methyl radical.

Freed[12] has first theoretically predicted the quantum rotation effect of a methyl group attached to $\dot{C}-R_2$ on the EPR spectra, which are characterized by the appearance of "E" lines. Also, the tunneling rotation of methyl hydrogens has been extensively studied by EPR spectroscopy.[13−18] For example, Davidson and Miyagawa[14] have explored the quantum effects of the tunneling rotation of the methyl group in $CH_3\dot{C}HR$, generated from L-alanine, on the EPR spectra. Geoffroy et al.[16] have studied the tunneling rotation of a hindered methyl group in X-ray-irradiated 2,2,5-trimethyl-1,3-dioxane-4,6-dione crystals. They evaluated a relatively accurate value of tunneling splitting (tunneling frequency) 830 ± 40 MHz by using ENDOR as well as ELDOR spectroscopy. The tunneling frequency of hindered rotation for the methyl group is determined by the barrier height of the hindering potential and the inertia of the rotor.[10]

Among possible inert gas matrixes, Ar (argon) is one of the most appropriate candidates to obtain EPR spectra with high resolution, mainly because it has no nuclear spin, including all stable isotopes. Even in Ar matrix, however, EPR spectra of the CH_3 radical reported earlier[4,5] did not distinctly reflect its intrinsic high resolution, because of super-hf splittings from iodine ^{127}I ($I = 5/2$) nuclei. Iodine is concomitantly generated with the CH_3 radical by photolysis of methyl iodide in the matrix. To prevent such unnecessary broadening of the EPR spectra due to interactions between the CH_3 radical and other radicals or molecules, used to generate the radical, we employed X-radiolysis of an Ar matrix containing only methane (CH_4, CD_4, and CH_2D_2) at 4.2 K. In this work, we present highly resolved EPR spectra of selectively deuterated methyl radical (CH_3, CD_3, CHD_2, and CH_2D) isolated in Ar, which were observed in the temperature range between 4.2 and 40 K. The temperature dependencies of "A" lines and/or "E" lines of CH_3 and CD_3 are discussed on the basis of a three-dimensional free

* To whom correspondence should be addressed.
[†] Hiroshima University.
[‡] Linköping University.
[§] University of Oslo.

10.1021/jp984716g CCC: $18.00
Published on Web 06/06/1999

quantum-rotor model. Several interesting quantum effects due to the coupling of motion to the spin degrees of freedom were newly observed. In contrast to the earlier works,[12−17] the hf coupling is anisotropic and no hindering barrier is present here. The system is analyzed in a direct product, spin-rotation basis set.

2. Experimental Section

Ar gas (Takachiho) as a matrix and CH_4, as well as deuterated methanes CD_4 (ICON) and CH_2D_2 (Isotec Inc.), were used without further purification. Their purities were 99.9999% for Ar and ≤97% for CH_4 and its two isotopomers. The D atom contents at the substituted positions for CD_4 and CH_2D_2 were 99% and 98%, respectively. The Ar mixed with 0.2 mol % methane was prepared in a Pyrex glass vessel (200 cm^3) attached with a Suprasil EPR sample tube (5 mm o.d., 20 cm long) by introducing Ar and methane gases separately up to at a total pressure of 600 Torr on a vacuum line. The mixed gaseous sample was condensed to form the solid solution at the tip of a tube immersed into liquid He. Alternatively, the solid solution sample was prepared by cooling the mixed gases down to 4.2 K with a temperature controller employing liquid He as a coolant, Oxford Cryostat ESR 900. The methyl radicals were generated by irradiating with X-rays (a Cu target with 60 kV, 50 mA electrons) the solid solution at 4.2 K for 30 min. The EPR spectra were usually recorded at microwave powers of 200 nW to 10 μW with a modulation width of 0.005 mT in the temperature range from 4.2 to 40 K on a Bruker ESP 300E spectrometer. The g values and hf splittings were calibrated employing a frequency counter 5350B (Hewlett-Packard) and a NMR gauss meter ER 035M (Bruker), respectively.

3. Experimental Results

3.1. Highly Resolved EPR Spectra of CH_3. Figure 1a shows the 6.0 K EPR spectrum of an Ar matrix containing 0.2 mol % of CH_4 immediately after X-ray irradiation at 4.2 K. The spectrum is narrow, with line width ca. 0.01 mT, and the high-resolution hf lines consist of a quartet with equal intensity, attributable to the "A" lines of CH_3 radical. The splitting of the "A" lines becomes slightly larger for the transitions with higher resonance field; i.e., the values 2.300, 2.315, and 2.330 mT were measured for the splitting between the resonance transitions, $m_F = 3/2$ and 1/2, 1/2 and −1/2, −1/2 and −3/2, respectively. The projection m_F corresponds to the z component $F_z = \Sigma_\nu I_{z;\nu}$ of the total nuclear spin $\mathbf{F} = \mathbf{I}_1 + \mathbf{I}_2 + \mathbf{I}_3$. The order of associated transitions is $m_F = 3/2$, 1/2, −1/2, and −3/2, from low to high field, because of the negative sign of the isotropic hf coupling. The above difference in the splittings of the "A" lines agreed with the value 0.015 mT expected from a second-order shift[19] at X-band, for ^{1}H with hf coupling $a(^1\mathrm{H}) = 2.315$ mT. On increasing the temperature above 12 K, two new lines, the "E" lines, appeared at the high-field side of the central $m_F = \pm 1/2$ peaks, both shifted by 0.024 mT from the "A" lines. Again, the difference in the resonance lines agreed well with the second-order shift between the multiplets $F = 3/2$ ("A" lines) and $F = 1/2$ ("E" lines).

The most striking observation regarding high resolution here is a series of small satellite multiplets superimposed on, almost hidden in the baseline of, the main spectra. The 20 K EPR spectrum, cf. Figure 1c, is shown again in Figure 2 after significant enhancement of the intensity scale. The multiplets are grouped into two next most probable CH_3 isotopomer combinations contained in the sample, considering the natural abundance of the atomic constituents, 1.1% for ^{13}C and 0.015% for D. One is a doublet of quartets with hf splittings of 3.860 and 2.315 mT, attributable to the $^{13}CH_3$ radical. The other is a triplet of triplets with splittings of 2.315 and 0.359 mT, attributable to the CH_2D radical. Such a high resolution suggests that the CH_3 and CH_2D radicals behave as if they were perfectly isolated from the host molecules of Ar matrix.

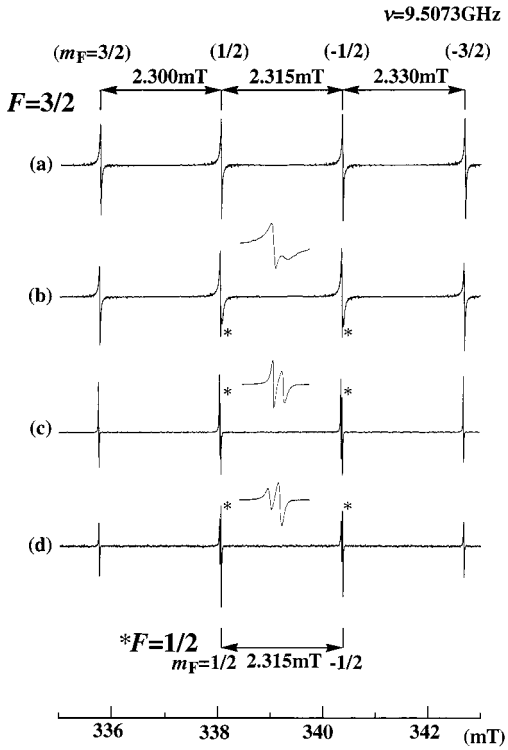

Figure 1. Temperature-dependent EPR spectra of CH_3 radical obtained in Ar matrix containing 0.2 mol % CH_4 after X-ray irradiation at 4.2 K: (a) 6 K, only the $F = 3/2$ quartet of "A_1" symmetry is observable; (b) 12.0 K; (c) 20.0 K; (d) 40.0 K, two $F = 1/2$ doublets of "E" symmetry marked as a star (*) increase in intensity as higher rotational levels are populated. The transitions of different symmetries ("A_1" and "E") are separated by a small second-order shift of the isotropic part of the hfc.

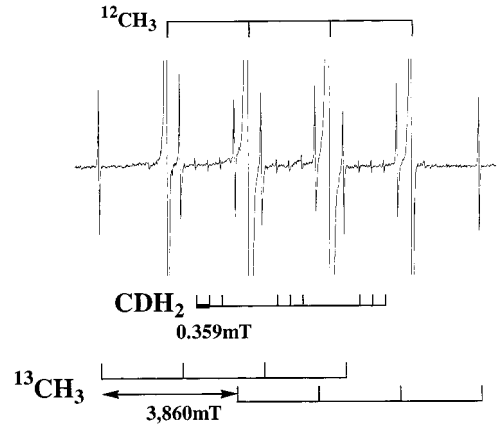

Figure 2. The 20 K EPR spectrum corresponding to Figure 1c obtained by significant enhancement of the intensity scale. The multiple isotope satellite peaks are disentangled as shown by the stick diagrams. The more intense double quartet is attributed to the $^{13}CH_3$ isotopomer combination, and the faint triple triplet is attributed to the CH_2D radical. The natural abundances of the magnetic isotopes in the sample are 1.1% (^{13}C) and 0.015% (D).

3.2. Temperature Dependence of EPR Line Shapes. The EPR line shape of CH_3 below 40 K was reversibly changed with temperature. Figure 3 shows the temperature dependence of the $m_F = 1/2$ EPR transition. When the temperature increased

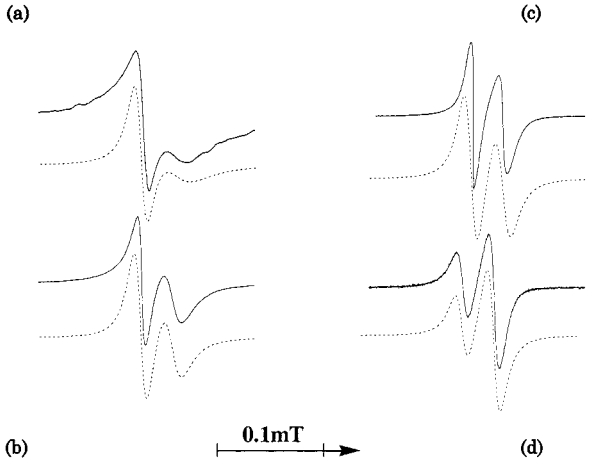

Figure 3. Temperature dependence of the "A_1" and the "E" lines at $m_F = +1/2$ for CH_3 in Ar matrix: (a) 12 K; (b) 16 K; (c) 20 K; (d) 40 K. A new broader transition ("E" line), compared to the original one ("A_1" line), appears at the high-field side of the latter, shifted by 0.024 mT. Its intensity is increasing with temperature; see further details in Figure 4.

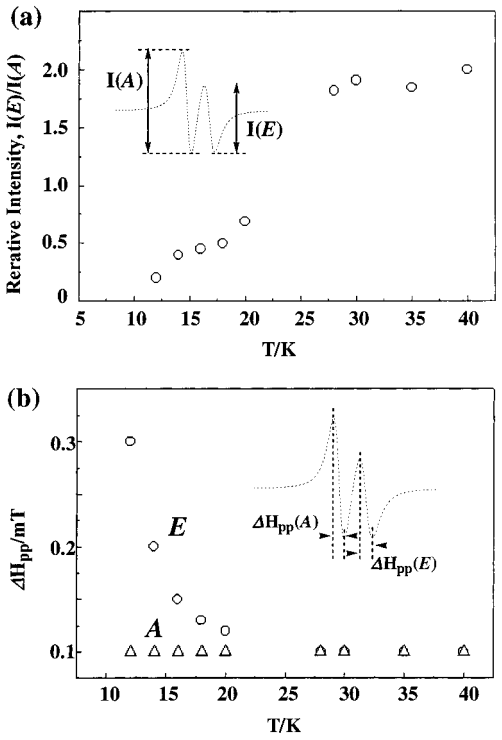

Figure 4. Temperature dependence of (a) the relative intensity of the "E" line to the "A_1" line and (b) the associated peak-to-peak line width (ΔH_{pp}) for the proton-rotor EPR spectrum. The intensities are approximate, were conveniently obtained by using the second derivatives, and do not exactly correspond to the absorption intensity; see details in text.

above 12 K, a new broader line, "E", became visible at higher field, shifted by ca. 0.024 mT from the original low-temperature "A" transition. The resonance position was in agreement with the second-order shift of the hf splitting. With further increasing temperature, the "E" lines increased in intensity. The relative peak intensity of the "E" lines to the "A" lines with projections $m_F = \pm 1/2$ finally reached a limiting value 2:1 at 40 K (Figure 4a). The temperature dependence of the peak growth and the line width of the peak will be explained in a later section of this paper in terms of a three-dimensional free rotor CH_3 dynamics.

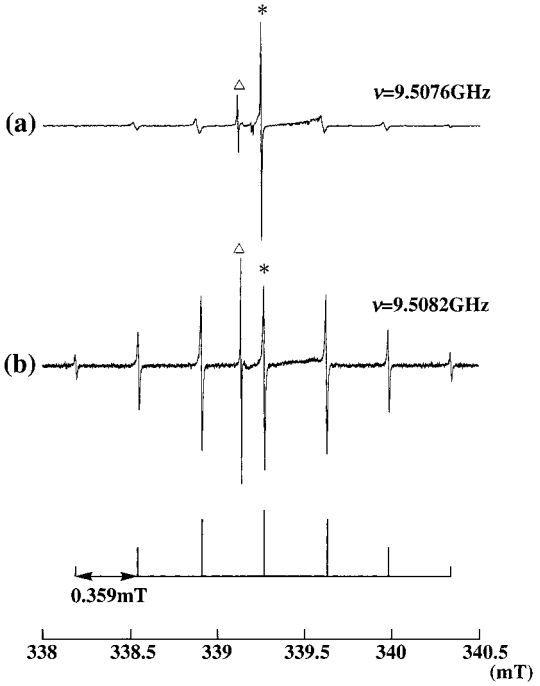

Figure 5. High-resolution EPR spectra of the CD_3 radical in Ar matrix at (a) 4.1 K and (b) 25.0 K. The strong central singlet in (a), marked by star (*), has relative intensity 105:1 to the outermost left transition. The odd line close to the center, marked by triangle (△), is the deuteron atom transition ($m_I = 0$), not relevant for this study.

To evaluate the experimental peak growth, the line shapes of the selected $m_F = 1/2$ transitions were simulated as follows. Each "A" line and "E" line of these transitions was independently reproduced by a Gaussian line shape with line width ΔH_{pp} (peak-to-peak distance of the first derivative spectrum) as an adjustable parameter. The simulated best-fit line shapes are shown in Figure 3 together with the experimental curves. The broadening is due to unresolved quantum splitting, as will be explained in the theoretical section. The ΔH_{pp} values giving the best fit are plotted versus temperature in Figure 4b. The line width of the "A" line, ΔH_{pp}(A), was found to be 0.01 mT irrespective of temperature, while at 4.2 K, the ΔH_{pp}(E) was 3 times larger than ΔH_{pp}(A). With increasing temperature above 28 K, ΔH_{pp}(E) decreased remarkably and reached the same value as ΔH_{pp}(A). Simultaneously, the relative peak intensity of the "E" to the "A" line grew almost linearly with temperature, as shown in Figure 4a, to the limiting value 2.

3.3. EPR Spectra of CD_3. Quantum effects on the EPR line shape were also discovered in perdeuterated methyl radical CD_3. Figure 5a shows the high-resolution EPR spectrum of the CD_3 radical in Ar matrix at 4.1 K. A septet with hf splitting 0.359 mT was observed. The splitting is 6.5 times smaller than of CH_3 radical, corresponding to the ratio of the magnetic moments of deuteron to proton. It is noteworthy to observe the strong intensity of the central peak with projection $m_F = 0$. The spectrum at 4.1 K exhibits a relative intensity ratio 1.0:3.8:7.0:105:8.7:4.3:1.5, which, except for the central line, is close to a "binomial" intensity distribution 1:3:6:7:6:3:1. This indicates that the observed CD_3 spectrum consists of a very strong transition at $m_F = 0$ superimposed on a "classical", high-temperature spectrum due to motional averaging. The central singlet is relatively narrow, with line width 0.006 mT, whereas the weaker outer transitions are about 4 times broader than the central singlet.

The relative intensity of the central line decreased rapidly with increasing temperature, and the spectral intensity reached

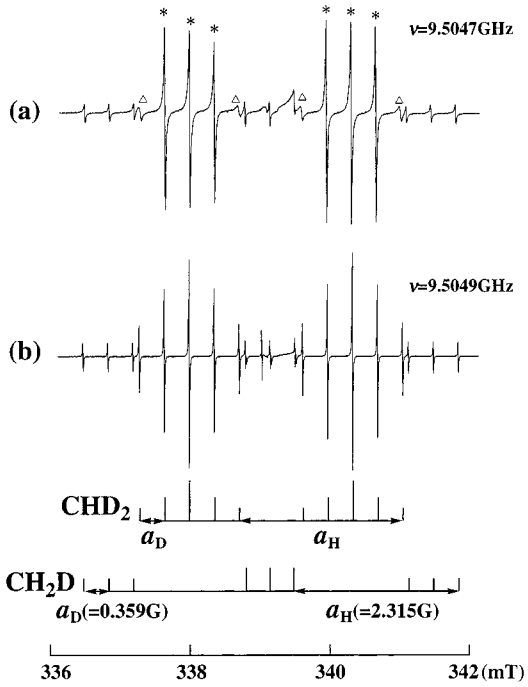

Figure 6. High-resolution EPR spectra of the CH_2D and CHD_2 radicals in Ar matrix at (a) 4.2 K and (b) 25.0 K, respectively. The strong triplet of CHD_2 at 4.2 K (*) has a relative intensity of ca. 10:1 to the associated outer two lines (△).

"binomial" distribution already at the relatively low temperature of 10 K; see Figure 5b. At the same time, all line widths converged to an identical value, ca. 0.009 mT. Obviously, the CD_3 spectra behaved much differently than CH_3 toward a temperature increase, reaching the fast motion limit more rapidly.

3.4. EPR Spectra of CH_2D and CHD_2. It is of interest to examine how the EPR spectra of partially deuterated methyl radicals, CHD_2 and CH_2D, behave at low temperatures. Therefore, these radicals were generated in Ar matrix by the same procedure as CH_3 and CD_3 (see the Experimental Section) but CH_2D_2 was used as a solute molecule instead of CH_4 and CD_4. A superposition of high-resolution spectra of CHD_2 and CH_2D radicals was clearly observed at 4.2 K, as shown in Figure 6a. Interestingly, their relative intensity ratio was ca. 8:1 = CHD_2/CH_2D, which is quite different from the unbiased statistical value 1:1. The result means that the light hydrogen, H, can be detached much more easily during dehydrogenation than the heavy hydrogen, D. The observed large deuterium isotope effect on the reaction is very characteristic of quantum mechanical tunneling.[20] The details will be the subject in a forthcoming paper.[21]

A double quintet with hf splittings 2.315 and 0.359 mT was observed for the CHD_2 radical at 4.2 K. Interestingly, the central triplet of each quintet was much stronger than the outer lines and had an intensity ratio of 1:1:1. Thus, the quintet intensity ratio is far from the "binomial" one 1:2:3:2:1, expected for the high-temperature spectrum. This indicates that the CHD_2 spectrum at 4.2 K was a superposition of stronger transitions at projections $m_F(D) = 1, 0, -1$ on a weaker, high-temperature spectrum of a freely rotating CHD_2. The central triplet transitions are relatively narrow with line width ca. 0.001 mT, whereas the two outer transitions are about 4 times as broad. Upon warming to 10 K, the relative intensity of the central triplet was changed to a "binomial" distribution 1:2:3:2:1; see Figure 6b. Concomitantly, all line widths converged to an identical value, ca. 0.001 mT. These observations correspond very well to the case of CD_3 radical.

The 4.2 K spectrum of CH_2D was a triple triplet due to the hf splittings of two hydrogen nuclei, major triplet, and one deuterium, minor triplets. The splittings were 2.315 and 0.359 mT, respectively, as in CHD_2. Instead of an expected binomial intensity distribution 1:2:1 of the major triplet due to the two equivalent protons, all lines were of equal intensity. However, in analogy to the case of CH_3 radical, upon warming above 15 K, a second line became visible at the high-field side of each of the transitions of the central triplet, shifted only by 0.024 mT. The relative intensity of the new lines with respect to the old reached the limiting value of 1:2 at 40 K; see Figure 6b.

4. Theoretical Analysis of Spectra

Certainly, the present case of unrestricted rotary motion resembles that of gas-phase EPR, but we have in addition the opportunity here to observe even the signal of frozen molecules almost under conditions of quantum isolation. Particular attention will be paid in the first two rotational levels $J = 0, 1$, which almost solely determine the quantum state characteristics of the lowest temperature spectra studied in this work.

Among the most surprising features of both the proton and the perdeuteron-rotor EPR spectra is the sharpness of the hf lines. Any characteristics of powder-like patterns are absent from the spectra. This property is mainly attributed to the quantum behavior of the system, meaning that, for the isolated, pure quantum-rotor model assumed, very few states are available for the system. Both rotary motion at low temperature and spin degrees of freedom in general share this property.

Another fact also contributes to the sharpness of the lines. In particular, it is amazing that all anisotropy disappears for the spectra observed at low temperatures close to 4 K. One normally expects a relatively large anisotropy, on the order of −2.0 mT[19] for α-protons assumed here (for deuterons × 1/6.5). On the contrary, theoretical calculations of the relevant dipole−dipole (d−d) matrix elements for the lowest rotational state $J = 0$ result in the inactive anisotropic part of the hf interaction. Only the multiplet hf structure, due to the pure scalar part $a = \mathrm{tr}\mathbf{A}/3$, is predicted to remain. For higher rotational levels with $J \geq 1$, where the d−d part of the hf coupling is active, if we consider a motionally averaged Hamiltonian, merely the scalar coupling is modified due to coupling to the motional degrees of freedom.

This behavior was confirmed by analytic computations and tested by preliminary simulations. The modification of the scalar part is shown best by averaging the secular part of the hf Hamiltonian for each isolated rotational level and finally calculating the spectrum in an approximate fashion, by adding the weighted spectra of these levels. Such a type of average is discussed in Zare.[22] Outlining the results, the average hf Hamiltonian for the $|J\ K\ M\rangle$ rotational level is given by

$$\langle H^{hfi}(\Omega)\rangle_{JKM} = [a + (1 - \delta_{J,0})C_{JKM}T_{zz}]S_zF_z \qquad (1)$$

where

$$C_{JKM} = \frac{[3K^2 - J(J+1)][3M^2 - J(J+1)]}{J(J+1)(2J+3)(2J-1)} \qquad (2)$$

and F_z is the z component of the total nuclear spin. The constants C_{JKM} are of the order of 1/10 for $J = 1$ and become smaller for higher rotational levels.

These relations show that the $J = 0$ level is influenced on average only by the unaltered isotropic part a. For higher levels,

SCHEME 1. A Rigid, Three-Dimensional, Symmetric-Top Rotor with D_3 Symmetry[a]

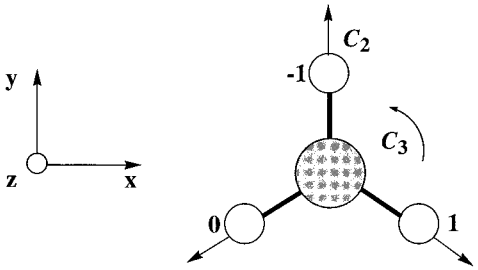

[a] The coordinate system and the rotation axes C_2 and C_3 are defined in a molecular frame of the CH_3 rotor. The labels of the protons are −1, 0, and 1.

a seemingly scalar interaction proportional to the *z* component of the dipole interaction $T_{zz} = A_{zz} - a$ must be added, which is very close to zero for α-protons. In combination with that, the onset of stochastic motion at higher temperatures shall average the anisotropic d−d part of the hf interaction that is traceless. The last observation gives a good explanation for the extreme sharpness of the spectrum at all measured temperatures, eventually rendering redundant the assumption by Morehouse et al.[3] of motional narrowing due to other kind of motions. In particular, even the next lower $J = 1$ rotation level will have a ca. 4 orders of magnitude larger rotational frequency (ca. 21 K; 4.2×10^4 MHz) than the hf anisotropy (ca. 30 MHz) for CH_3. Furthermore, by the same argument, it is expected that not only the dipolar part of the hf interaction but also any other anisotropic interactions based on second-order tensorial quantities, such as the nuclear quadrupole interaction, will be diminished at the lowest rotational level.

4.1. CH_3 Rotor. The equal intensity of the well-known lowest-temperature quartet[12] indicates involvement of only the rotational ground-state quartet[1] with $J = 0$, a state referred to here as *stopped quantum rotor*. The four accompanying totally symmetric A_1 states are

$$\Psi^{A_1}_{n,n,n}(0\,0\,0) = |0\,0\,0\rangle|n\,n\,n\rangle$$
$$\Psi^{A_1}_{n,n',n}(0\,0\,0) = \frac{1}{\sqrt{3}}|0\,0\,0\rangle[|n'\,n\,n\rangle + |n\,n'\,n\rangle + |n\,n\,n'\rangle] \quad (3)$$

for $n = -n' = \pm 1/2$.

In the above expression and in the following text, a general unperturbed mixed spin-rotation $R \otimes I$ basis function will be designated by $\Psi^{\Gamma}_{n_{-1}n_0n_1}(J\ K\ M)$, where $\Gamma = A_1$ or A_2 is the overall symmetry of this function, and an irreducible representation of the D_3 group. A model of the CH_3 radical is shown in Scheme 1. The nuclear projections are n_j while *J*, *K*, and *M* are the rotational quantum numbers of the basis function.

The presence of E lines aside the A_1 lines, first at a temperature of 12 K and higher, appears as delicate splitting of the central $m_F = \pm 1/2$ doublet, as it is shown in Figure 1. The relative intensity of the E line increases gradually with temperature and stabilizes at higher temperatures, as it is shown in Figure 4a. At low temperatures, it is expected that quantum effects, in the form of a scalar shift between the A and E lines for the first few rotational levels, give the experimental shift in Figure 4b. At higher temperatures, this interaction is transferred to second-order shift by rotational averaging of the hf interaction. The coupling of mixed $R \otimes I$ states within the degenerate *M* manifolds by the anisotropic part of the hyperfine interaction introduced when $J \geq 1$ is the reason for the differential broadening of the EPR transitions. Indirectly also, this coupling leads to small variation of the A−E splitting of the central $m_F = \pm 1/2$ transitions before the temperature reaches 12 K. This coupling was verified analytically[23] for electron S-spin secular Hamiltonian within the $\{J = 1, |K| = 1, |M| \leq 1\}$ block of the CH_3 rotor, but the broadening is more prominent in the experimental CD_3 and CHD_2 spectra, as shown in Figures 5a and 6a.

All the possible states of this manifold are

$$\Psi^{A_1}_{n,n',n}(1\ q\ M) = \frac{1}{\sqrt{6}}[|1\ q\ M\rangle + |1\ -q\ M\rangle]\sum_{\nu}\epsilon_{\nu}^{-q}|\zeta_{\nu}\rangle \quad (4)$$

with $n = -n' = \pm 1/2$ and with $q = \pm|K|$. The even permutations $|\zeta_{\nu}\rangle$ of the nuclear projections used in the above definition are given by the following equations:[1]

$$|\zeta_0\rangle \equiv |n_-\,n_0\,n_+\rangle$$
$$|\zeta_+\rangle \equiv |n_+\,n_-\,n_0\rangle \quad (5)$$
$$|\zeta_-\rangle \equiv |n_0\,n_+\,n_-\rangle$$

The complex coefficients ϵ_{ν}^{q} are given by

$$\epsilon_{\nu}^{q} = \exp(i\nu q 2\pi/3) \quad (6)$$

In the earlier study of β-proton rotors,[1] the scalar interaction of a quadratic cosine form couples the degenerate rotational states with projections $J_z = \pm 1$ and split them, giving the characteristic triplet called "E" lines.[12] We can say that here the "E" lines are almost superimposed to the "A" lines mainly due to that the dominant scalar part of the hf interaction is not depending on rotation. The dipolar part should give here an analogous splitting to that of the "E" lines. However, in the Pauli-adapted basis set, symmetrized according to D_3 point group, the molecular projection of the angular momentum $J_z = K$ for three-dimensional rotation is no longer a good quantum number. Its place is taken by the laboratory projection $J_Z = M$; see, for example, eq 4. At last, for really high temperatures, when ideally all rotational states contribute to motion, the averaged hf interaction transfers to regular second-order splitting. The experimental value 0.024 mT is confirmed by a simple calculation.

4.2. CD_3 Rotor. The most striking characteristic of the EPR line shape is the abnormally strong central transition at the lowest experimental temperature 4.1 K. Only a single basis function, namely,

$$\Psi^{A_2}_{-1,0,1}(0\,0\,0) = \frac{1}{\sqrt{6}}|0\,0\,0\rangle\{[|-1\,0\,1\rangle + |1\,-1\,0\rangle + |0\,1\,-1\rangle] - [|1\,0\,-1\rangle + |-1\,1\,0\rangle + |0\,-1\,1\rangle]\} \quad (7)$$

is allowed by the Pauli principle for the lowest rotational level $J = 0$. This is the only possible mixed $R \otimes I$ state, containing the antisymmetric nuclear spin wave function. The result is in severe contrast to the expected 1:1:2:3:2:1:1 intensity distribution, as, for example, in the case of the β-proton rotors with C_3 symmetry, where the symmetric nuclear basis wave functions were used.[1] It was found in the present study that the electronic state has to be included in the application of the Pauli principle[12,23] in order to obtain correct overall exchange symmetry for bosons.

For the same reason as in the proton-rotor spectrum, the expected "E" lines do not shift from their original positions but superimpose on the "A" lines. In particular, the second-order

effects are not of significance for deuterons because of the smaller hf splitting. In fact, no such shifts were visible even at the highest temperatures. It is not strange that the deuteron-rotor spectrum becomes very similar to the classical, fast-motion spectrum already at a temperature as low as 6 K. The intensity distribution calculated using only the allowed unperturbed $R \otimes I$ wave functions for the $J = 1$ level reveals the pattern 1:3:6:4:6:3:1, which is almost identical to the classical one, except for the weaker central line. However, the intensity of the central line is more than compensated by the transition from the lowest rotational level $J = 0$, as it was shown above. Another reason for the faster transition of the spectrum to classical appearance is that the energy difference of the rotational levels in deuteron rotor is smaller, compared to proton rotor, and therefore the higher levels are more easily populated as the thermal energy of the system increases.

The unperturbed mixed *spin-rotation* wave functions for the $J = 1$ level are given by

$$\begin{aligned}\Psi^{A_2}_{n,n,n}(1\ 0\ M) &= |1\ 0\ M\rangle|n\ n\ n\rangle \\ \Psi^{A_2}_{n,n',n}(1\ 0\ M) &= \frac{1}{\sqrt{3}}|1\ 0\ M\rangle[|n'\ n\ n\rangle + |n\ n'\ n\rangle + |n\ n\ n'\rangle]\end{aligned} \tag{8}$$

for n and $n' = 0, \pm 1$, that amounts to $3 + 6 = 9$ basis wave functions, with M degeneracy excluded. Together with the following one:

$$\begin{aligned}\Psi^{A_2}_{-1,0,1}(1\ 0\ M) = \frac{1}{\sqrt{6}}|1\ 0\ M\rangle[&|-1\ 0\ 1\rangle + |1\ -1\ 0\rangle + \\ &|0\ 1\ -1\rangle + |1\ 0\ -1\rangle + |-1\ 1\ 0\rangle + |0\ -1\ 1\rangle]\end{aligned} \tag{9}$$

they constitute the $K = 0$ manifold of the $J = 1$ level.

For completeness, we even give further the rest of the symmetrized A_2 wave functions of the $J = 1$ level obtained for $|K| = 1$.

$$\begin{aligned}\Psi^{A_2}_{n,n',n}(1\ q\ M) &= \frac{1}{\sqrt{6}}[|1\ q\ M\rangle - |1\ -q\ M\rangle]\sum_j \epsilon_j^{-q}|\zeta_j\rangle \\ \Psi^{A_2}_{n_{-1},n_0,n_1}(1\ q\ M) &= \\ &\frac{1}{\sqrt{6}}[|1\ q\ M\rangle\sum_j \epsilon_j^{-q}|\zeta_j\rangle - |1\ -q\ M\rangle\sum_j \epsilon_j^{q}|\xi_j\rangle]\end{aligned} \tag{10}$$

For $q = \pm 1$, here we count, $6 + 2 = 8$ more states for the last block, with M degeneration excluded. Notice that the last basis function is rather unusual since it is not possible to factorize in individually symmetrized rotational and nuclear spin parts. The odd permutations $|\xi_j\rangle$ necessary for the definition of the last equation are given by[23]

$$\begin{aligned}|\xi_0\rangle &\equiv |n_+\ n_0\ n_-\rangle \\ |\xi_+\rangle &\equiv |n_0\ n_-\ n_+\rangle \\ |\xi_-\rangle &\equiv |n_-\ n_+\ n_0\rangle\end{aligned} \tag{11}$$

4.3. CHD_2 and CH_2D Rotors. The most interesting observation about the CHD_2 EPR line shape at 4.2 K is the abnormally strong 1:1:1 triplet due to the two deuterons; see Figure 6. The triplet can be attributed to the following three functions:

$$\begin{aligned}\psi^B_{-1} &= [|-1\ 0\rangle - |0\ -1\rangle]/\sqrt{2} \\ \psi^B_{1} &= [|0\ 1\rangle - |1\ 0\rangle]/\sqrt{2} \\ \psi^B_{0} &= [|1\ -1\rangle - |-1\ 1\rangle]/\sqrt{2}\end{aligned} \tag{12}$$

Only the deuteron-spin projections are given in the above expressions for simplicity. These antisymmetric, nuclear-spin wave functions are the only ones allowed by the Pauli principle for the lowest rotational level $J = 0$, and they correspond to a B irreducible representation regarding the C_2 symmetry of CHD_2.

Further, it is enough for the purpose of the present work to outline the properties of the $J = 1$ level for the particular rotational z projection $K = 0$ of the radical. (The other projections give similar distribution.) There are six possible nuclear-spin, totally symmetric combinations for CHD_2 allowed in this level. They are

$$\begin{aligned}\psi^A_{-2} = |-1\ -1\rangle \quad \psi^A_0 = |0\ 0\rangle \quad \psi^A_2 = |1\ 1\rangle \\ \psi^A_{-1} = [|-1\ 0\rangle + |0\ -1\rangle]/\sqrt{2} \\ \psi^A_{1} = [|0\ 1\rangle + |1\ 0\rangle]/\sqrt{2} \\ \psi^A_{0} = [|1\ -1\rangle + |-1\ 1\rangle]/\sqrt{2}\end{aligned} \tag{13}$$

They comprise an approximate 1:1:2:1:1 D hf pattern for the $J = 1$ level, and when superimposed on the B lines of the $J = 0$ level, because of the negligibly small second-order shifts, they reach the fast rotation intensity distribution 1:2:3:2:1. Similarly to the case of the CD_3 radical, the $J = 1$ levels are easily populated as the temperature increases. In fact, the spectrum reaches classical appearance at the relatively low temperature of 10 K.

In a similar manner, the major triplet of CH_2D with equal intensity can be easily attributed to totally symmetric A nuclear-spin states (in C_2) of two protons with $F = 1$. Knight et al.[24] have observed similar nuclear spin states for H_2O^+ radical cation isolated in Ne matrix at low temperatures close to 4 K.

This short account of the mixed rotors does not exhaust the topic that is also interesting due to the similarity of the above mixed H-,D-rotor radicals to other important radicals. In contrast to the pure H and D rotors, this system is not a symmetric top and treatment of the rotational degree of freedom becomes more involved. Furthermore, many other systems dispose the low C_2 symmetry required for quantum effects and can behave similarly. A more thorough investigation is in process.[23]

5. Conclusions

The present study deals systematically with all possible combinations of methyl radicals and selectively deuterated species, CH_3, CD_3, CHD_2, and CH_2D, isolated in argon matrix and the quantum effects of their EPR line shapes close to 4 K. Also, the temperature dependence of the line shapes exhibits clear quantum effects. The quantum effects are due to spin-rotation couplings by the anisotropic part of the hf interaction and are visualized as abnormal intensity distributions of the resonance lines and very sharp EPR transitions. The sharpness of the experimental spectra is due to effectively averaged anisotropic hf interaction, even for stopped rotor. In particular, the stopped rotor, i.e., the $J = 0$ state, that dominates the lowest temperature spectra was shown to be free from the dipole−dipole hyperfine interaction, while this anisotropic part shall

be efficiently averaged by rotation at elevated temperatures due to population of higher rotational states. The anisotropy of the hf interaction had to be deduced indirectly from the presence of quantum effects necessitating a source of spin-rotation coupling. This may be the reason no anisotropic coupling parameters of these systems are known in the literature.

Theoretical analysis based on the following assumptions could reproduce the fundamental quantum effects observed experimentally: (a) planar D_3 geometry for CH_3 and CD_3 and a planar C_2 geometry for CH_2D and CHD_2; (b) three-dimensional quantum rotation; (c) thermally isolated radical.

Application of the Pauli principle in combination to the operations of D_3 or C_2 point groups resulted in interesting selections for ESR transitions for the CH_3 and CD_3, as well as CH_2D and CHD_2, spectra, respectively, in particular for the stopped quantum-rotary state $J = 0$. That is, the hf quartet of CH_3 radical was attributed to the four possible proton-spin states with symmetry A_1 in the D_3 point group. The central strong singlet of CD_3 was attributed to the only possible deuteron-spin state with symmetry A_2 in D_3. The abnormally strong 1:1:1 triplet of CHD_2 was attributed to the three possible deuteron-spin states of C_2 with B symmetry.

Such severe restrictions of possible nuclear states in the lowest levels might cause unexpected effects on the electron spin relaxation for free rotors that are missing tunneling, the other possible source of electron relaxation at very low temperatures. A more extended account of the theory together with quantitative analysis of the temperature-dependent EPR line shapes is in preparation to be published in a forthcoming work.[23]

Acknowledgment. This work was supported by the Swedish Foundation for International Cooperation in Research and Higher Education (STINT) and a Subsidy of Science Research of Japanese Ministry of Education (Grant 08240105). We thank Prof. Anders Lund for his helpful discussion and support.

References and Notes

(1) Sørnes, A. R.; Benetis, N. P. *Chem. Phys.* **1998**, *151*, 226.

(2) Jen, C. K.; Foner, S. N.; Cochran, E. L.; Bowers, V. A. *Phys. Rev.* **1958**, *112*, 1169.

(3) Morehouse, R. L.; Christiansen, J. J.; Gordy, W. *J. Chem. Phys.* **1966**, *45*, 1751.

(4) Kasai, P. H.; McLeod, D., Jr. *J. Am. Chem. Soc.* **1972**, *94*, 7975.

(5) Cirelli, G.; Russu, A.; Wolf, R.; Rudin, M.; Schweiger, A.; Günthard, H. H. *Chem. Phys. Lett.* **1982**, *92*, 223.

(6) Fujimoto, M.; Gesser, H. D.; Garbutt, B.; Cohen, A. *Science* **1966**, *154*, 381.

(7) Shiotani, M.; Yuasa, F.; Sohma, J. *J. Phys. Chem.* **1975**, *79*, 2669.

(8) Fessenden, R. W. *J. Phys. Chem.* **1964**, *71*, 74.

(9) Kubota, S.; Iwaizumi, M.; Ikegami, Y.; Shimokoshi, K. *J. Chem. Phys.* **1979**, *71*, 4774.

(10) Sørnes, A. R.; Benetis, N. P.; Erickson, R.; Mahgoub, A. S.; Eberson, L.; Lund, A. *J. Phys. Chem. A* **1997**, *101*, 8987.

(11) McConnel, H. M. *J. Chem. Phys.* **1958**, *29*, *1472*.

(12) Freed, J. H. *J. Chem. Phys.* **1965**, *43*, 1710.

(13) Clough, S.; Poldy, F. *J. Chem. Phys.* **1969**, *51*, 2076.

(14) Davidson, R. B.; Miyagawa, I. *J. Chem. Phys.* **1970**, *52*, 1727.

(15) Clough, S.; Hill, J. R. *J. Phys. C: Solid State Phys.* **1974**, *7*, L20.

(16) Geoffroy, M.; Kispert, L. D.; Hwang, J. S. *J. Chem. Phys.* **1979**, *70*, 4238.

(17) Matsushita, M.; Momose, T.; Shida, T. *J. Chem. Phys.* **1990**, *92*, 4749.

(18) Kubota, S.; Matsushita, M.; Shida, T.; Abu-Raqabah, A.; Symons, M. C. R.; Wyatt, J. L. *Bull. Chem. Soc. Jpn.* **1995**, *68*, 140.

(19) Atherton, N. M. *Principles of Electron Spin Resonance*; Ellis Horwood Ltd.: West Sussex, England, 1993.

(20) Benderskii, V. A.; Makarov, D. E.; Wight, C. A. *Chemical Dynamics at Low Temperatures, Advances in Chemical Physics*; John Wiley and Sons: New York, 1994; Vol. LXXXVIII.

(21) Shiotani, M.; Komaguchi, K. Manuscript in preparation.

(22) Zare, R. N. In *Angular Momentum. Understanding Spatial Aspects in Chemistry and Physics*; John Wiley & Sons: New York, 1988.

(23) Benetis, N. P.; Sørnes, A. R.; Shiotani, M.; Komaguchi, K.; A. R.; Yamada, T. Manuscript in preparation.

(24) Knight, L. B., Jr.; Steadman, L. *J. Chem. Phys.* **1983**, *78*, 5940.